

Long Video Understanding with Learnable Retrieval in Video-Language Models

Jiaqi Xu, Cuiling Lan, Wenxuan Xie, Xuejin Chen, Yan Lu

Abstract—The remarkable natural language understanding, reasoning, and generation capabilities of large language models (LLMs) have made them attractive for application to video understanding, utilizing video tokens as contextual input. However, employing LLMs for long video understanding presents significant challenges. The extensive number of video tokens leads to considerable computational costs for LLMs while using aggregated tokens results in loss of vision details. Moreover, the presence of abundant question-irrelevant tokens introduces noise to the video reasoning process. To address these issues, we introduce a simple yet effective learnable retrieval-based video-language model (R-VLM) for efficient long video understanding. Specifically, given a question (query) and a long video, our model identifies and selects the most relevant K video chunks and uses their associated visual tokens to serve as context for the LLM inference. This effectively reduces the number of video tokens, eliminates noise interference, and enhances system performance. We achieve this by incorporating a learnable lightweight MLP block to facilitate the efficient retrieval of question-relevant chunks, through the end-to-end training of our video-language model with a proposed soft matching loss. Our experimental results on multiple zero-shot video question answering datasets validate the effectiveness of our framework for comprehending long videos.

Index Terms—Large Language Models, Long Video Question Answering, Retrieval-based Video-language Model.

I. INTRODUCTION

WITH the rapid development of the Internet and the widespread use of cameras and smartphones, both individuals and businesses are generating massive amounts of video data every day in various fields such as entertainment, education, and technology. In such era of information explosion, understanding and extracting information from video content has become increasingly important to better meet people's needs and promote social progress. In this context, Video Question Answering (video QA) emerges as an essential interface for extracting and delivering information from video content. Video QA systems allow users to ask natural language questions about videos and receive answers based on the visual (and auditory) information within the video.

There is a growing trend towards leveraging large language models (LLMs) for video QA [1]–[4]. On one hand, LLMs benefit from the vast knowledge acquired through training

J. Xu is with the School of Information Science and Technology, University of Science and Technology of China, Hefei 230026, China. E-mail: xujiaqi@mail.ustc.edu.cn

C. Lan, W. Xie and Y. Lu are with the Microsoft Research Asia, Beijing 100080, China. E-mail: {culan, wenxie, yanlu}@microsoft.com

X. Chen is with the School of Information Science and Technology, University of Science and Technology of China, Hefei 230026, China. E-mail: xjchen99@ustc.edu.cn

This work was done when J. Xu was an intern at Microsoft Research Asia.

on enormous text corpora; on the other hand, they provide users with a more natural and intuitive way to interact with video data. Generally, visual tokens extracted from a video snippet are transformed and used as input (prompt) to the LLM, along with the text query. However, it is worth noting that the consumption of abundant visual tokens by a LLM can significantly increase the memory and computational burden, making it unaffordable for low-resource GPU agents. To mitigate this issue, Video-ChatGPT [1] performs global spatial and temporal pooling on the video tokens, although this comes at the cost of losing detail due to pooling. Video-LLaMA [4] aggregates video tokens using a Q-former with cross attention. Most of these methods are designed for short-video QA tasks, where answer-related frames usually spread over the trimmed video snippet.

In practical application scenarios, users often raise questions about long videos (*e.g.*, longer than 1 minute), in which the segments that are relevant to the questions usually constitute only a small fraction of the entire video. The presence of answer-irrelevant segments constitutes redundancy and can potentially interfere with the video QA process, thus reducing its effectiveness. Therefore, it is imperative to develop a simple yet efficient framework for long video QA.

To address these challenges, we draw inspiration from biology and cognitive science. As we know, human working memory is a cognitive system responsible for temporarily holding and manipulating information necessary for complex tasks such as reasoning, learning, and comprehension [5]. Faced with the vast amount of information stored in long-term memory, working memory selectively retrieves relevant information while filtering out irrelevant data for further cognition. Motivated by this, we aim to design a framework that is capable of identifying and concentrating on relevant video segments while filtering out irrelevant information, ensuring accurate and efficient question answering without imposing excessive computational demands.

In this paper, we propose a retrieval-based video-language model, R-VLM, for effective long-video question answering. Fig. 1 shows the overall framework. Specifically, given a long video and a question (query), we divide the video into a sequence of non-overlapping video chunks, with each chunk representing a short video segment (*e.g.*, 4 seconds). Note that we sample at a low frame rate in considering the memory limitation and video redundancy. To allow a chunk to contain dynamic temporal information, we use 4 seconds that are expected to contain temporal dynamics as the chunk unit. We then aggregate the encoded tokens within a chunk through spatial and temporal pooling to obtain chunk tokens, reducing redundancy while preserving considerable local details. We

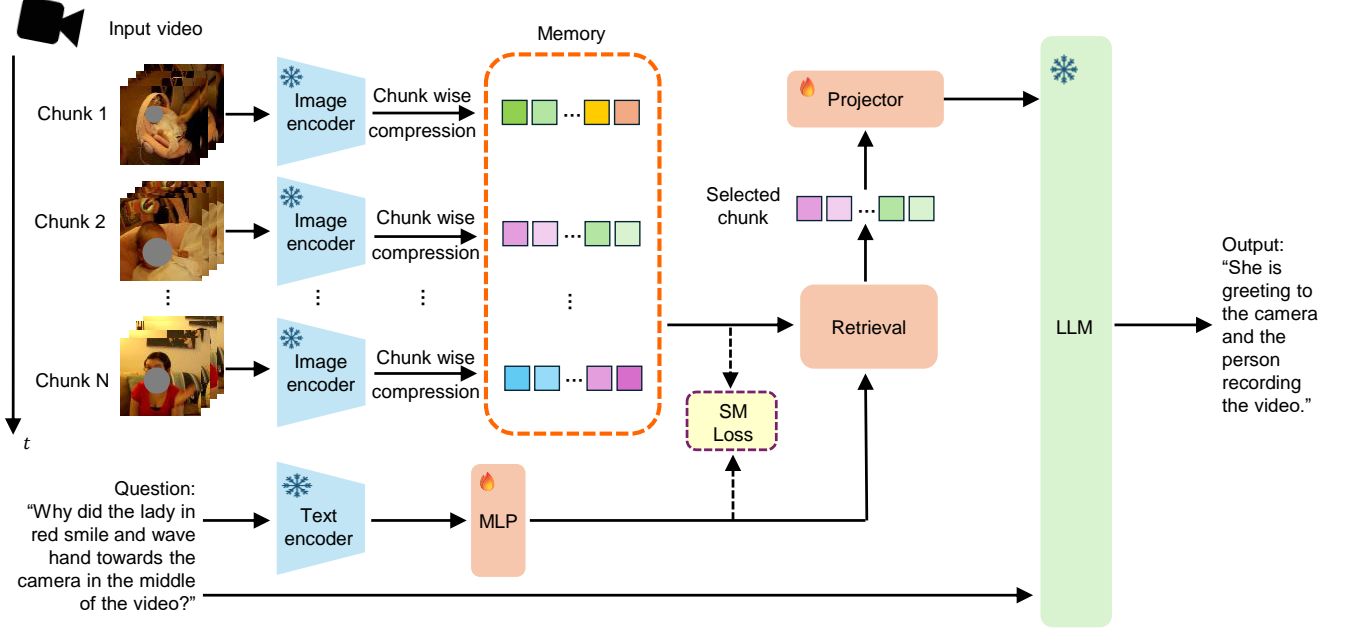


Fig. 1: Illustration of our learnable retrieval-based video-language model for efficient long video question answering. We encode an input long video into a sequence of video chunks, with each chunk represented by a set of spatial and temporal visual tokens. Question-guided retrieval is performed to find the top K relevant video chunks, with their tokens as the input to the LLM for answer generation. Here, we use $K = 1$ for illustration purpose. A learnable lightweight MLP block (following the text encoder) and the projector are trained end-to-end, where the encoders and LLM are frozen. Soft matching (SM) loss is introduced to regularize the retrieval related learning.

perform question-guided retrieval by introducing a lightweight *learnable MLP block* on top of a CLIP text encoder to obtain the top K most relevant chunks, and subsequently use the small set of tokens (after projection) from these chunks as input to the LLM for video reasoning. In this way, we efficiently match and pass the most question-pertinent visual information to the LLM for inference.

Our framework demonstrates superior zero-shot generalization performance on multiple video QA datasets,

Our contributions can be summarized below:

- We propose a learnable retrieval-based video-language model for effective long video understanding.
- We validate the feasibility of using learnable lightweight retrieval for selecting the most question-relevant video chunks to answer questions from a long video, within large video-language model in an end-to-end manner.
- Our method achieves superior performance and the ablation studies demonstrate the superiority of our retrieval mechanism.

II. RELATED WORK

Video Question Answering (Video QA) has emerged as a crucial task for extracting information from videos through natural language interactions. Before the prevalence of LLM, conventional methods focus on network and multi-modal interaction designs for video understanding [6]–[13]. Yuan *et al.* [6] propose AMN to learn multi-modal feature representations by finding a more coherent subspace for video clips and

the corresponding texts based on GANs. Wang *et al.* [7] propose an alternating attention network, which iteratively focuses on frame regions, video frames, and words in the question in multi-turns to generate better joint representations of the video and question. DualVGR [8] uses a multi-view graph attention network to provide a context-aware feature representation. A query punishment module is applied to modulate irrelevant visual features through multiple reasoning cycles to reduce their interference. Qian *et al.* [9] propose a scheme to localize the question to a segment in the video to infer the answer, where a 3DCNN network and attention modules are designed to extract features and generate location proposals. Based on existing LLM and visual encoder, how to design a simple framework that can leverage the LLM and visual encoder for long video understanding is still under-explored. We propose R-VLM that leverage a lightweight MLP block to enable a learnable retrieval module for efficient video question answering.

Recent advances in LLMs have inspired and promoted the integration of pre-trained LLMs with visual processing components for multimodal understanding [14], [15], [16], [17], [18], [19]. Flamingo [14] and BLIP-2 [15] are seminal works that leverage the pre-trained LLM and CLIP image encoder for zero-shot image-text abilities. BLIP2 [15] introduces a Q-Former to map the image tokens from the CLIP encoder [20] to the textual embedding space of LLMs. InstructBLIP [21] uses instruction-aware Q-Former to globally aggregate the visual tokens. LLaVA [17] maps the image spatial tokens

to the textual embedding space of LLMs using a linear projector. LLaVA [17], MiniGPT4 [16], and mPLUG-owl [22] promote instruction following using image-instruction-following datasets.

Some works have focused on enabling video-language understanding by integrating vision encoder and LLMs [23], [1], [3], [2]. Video-LLAMA [23] uses a video Q-former to assemble the features from the pre-trained CLIP image encoder. Video-ChatGPT [1] performs spatial and temporal pooling of the feature maps encoded by the pre-trained CLIP image encoder. The ensembled visual tokens are taken as input to the LLMs. Most of these works globally aggregate video tokens. They may work well for short videos. But for the long video-language comprehension, they would be less efficient. The information of the question-related video segments may be submerged to the global-wise token representations, making the reasoning difficult.

SeViLA [24] utilizes the BLIP-2 image-language model for selecting temporal key frames which are subsequently inputted into BLIP-2 for video-based question answering. The process involves complex training for convergence and the frame selection is computationally expensive due to the necessity of processing potential frames through the large BLIP-2 model (with even the smallest version being 3.1 billion parameters). This would not be suitable for long video understanding.

In order to understand long videos, MovieChat [25] leverages short-term and long-term memories for video representation. LLaMA-VID [26] represents every frame coarsely by two tokens to reduce the computation and memory cost for long video reasoning, which however still introduces temporal redundancy and interference in LLM inference. SeViT [27] proposes a framework for long untrimmed video understanding. It includes a non-parametric frame retriever to select a few query-relevant frames from the video and uses them as the input to a video-grounded text generator. However, the frame selector is non-parametric and the system cannot be end-to-end optimized, resulting in the inferiority of the selected frames and sub-optimal performance. Different from SeViT, we introduce learnable retrieval through a light-weighted MLP block for building an end-to-end video-language model, powered by LLM. In [28], a Frame-Prompter is designed to select key video frames. However, with only video frames as input to the Frame-Prompter, the selection is not question aware and would lead to ineffective. Wang *et al.* [29] fuse the question-and-answer pairs as event descriptions to find keyframes as target moments and pseudo-labels. Unlike [29], we do not use pseudo-labels for supervision. Our framework leverages the end-to-end learning to automatically select the question-relevant chunks, providing a large optimization space and avoiding the side effects from the inaccuracy of pseudo-labels. VideoTree [30] extracts query-relevant information from the input video through an iterative process, based on their relevance to the query scored by an LLM. However, leveraging an additional LLM for key frame selection increases the complexity of the system. In contrast, our retrieval design is lightweighted and end-to-end trained in the VLM.

III. RETRIEVAL-BASED VIDEO-LANGUAGE MODEL

Given a lengthy video, it is time-consuming to watch the entire content to obtain the desired information. A video understanding system, which can automatically infer answers based on the long video and user's query (question), is in high demand. LLMs possess extensive world knowledge and reasoning capabilities, albeit at the expense of high computational complexity. Some previous works on multi-modal language models utilize a set of projected visual tokens as input (context) to LLM for inference [15], [16], where the inference cost is proportional to the number of input visual tokens.

Leveraging powerful LLMs to understand long videos presents challenges. Firstly, we expect to use only a small set of tokens as input to reduce computational costs. Secondly, as the video length increases, in general, there is a corresponding growth in the number of visual tokens and the overall amount of information. Representing a long video with very few tokens becomes difficult. Furthermore, question-irrelevant information may interfere with reasoning. Motivated by the retrieval mechanism of brain, we introduce a question-guided retrieval mechanism to identify and select a few relevant video chunks as context of LLM.

Fig. 1 illustrates the overall framework of our proposed retrieval-based video-language model (R-VLM), designed for efficient long video understanding. The framework is comprised by several components: a frozen LLM, a frozen image encoder, a frozen text encoder, a memory for storing video chunk tokens, a retrieval module for selecting the question-relevant chunks, a learnable MLP block, and a projector. Through end-to-end training with cross-entropy loss and the proposed soft matching (SM) loss, the MLP block is optimized to learn to identify the most relevant K chunks, while the projector is optimized to align the selected visual tokens with the text (question) space. In the following subsections, we provide a detailed explanation of the key components and designs.

A. Video Tokenization

Video tokenization involves encoding the raw video into visual tokens, which will be processed and then passed to the LLM for inference. We partition a long video into chunks, with each chunk represented by a set of compressed visual tokens. Such chunk tokens are stored in a memory to facilitate question-guided retrieval for efficient video question-answering.

Chunking the video and feature extraction Given a long video sample $V_i \in \mathbb{R}^{T_i \times H \times W \times 3}$ with T_i frames, height H , and width W , we divide it into small non-overlapped video chunks (see Fig. 1), which are the basic units with each containing spatial information and temporal dynamic for question-guided retrieval. We set the duration of a chunk to 4 seconds, *i.e.*, $M = 4$ frames when frame rate is 1 frame per second (fps). We have $L_i = \lceil T_i/M \rceil$ chunks, where $\lceil \cdot \rceil$ denotes the ceiling function.

We adopt the pretrained language-image model CLIP [20] to extract per frame visual token features. For the j^{th} video

chunk $V_i^j \in \mathbb{R}^{M \times H \times W \times 3}$, we obtain $M \times h \times w$ visual tokens $F_i^j \in \mathbb{R}^{M \times h \times w \times D}$ from the CLIP vision encoder, where $h = H/p$, $w = W/p$, D denotes the number of channels. p denotes the patch size ($p = 14$ for ViT-L/14, $h = 16$, $w = 16$).

Chunk wise compression The preliminary token number of a chunk is large, which would result in a high computational burden and large memory requirement for the LLM even though we only select a few chunks as input to LLM. Therefore, we perform chunk-wise pooling to obtain reduced spatial and temporal tokens (see Fig. 3 for the illustration in Supplementary Section A).

Particularly, we found that reducing the spatial resolution by a factor of 4 leads to marginal difference in performance while this can significantly reduce the number of tokens by 75%. Therefore, we perform spatial average pooling with stride 2 to have $M \times \bar{h} \times \bar{w}$ tokens per chunk, where $\bar{h} = h/2$ and $\bar{w} = w/2$. This is equivalent to taking the CLIP features of reduced resolution as the extracted feature.

How to further reduce the number of tokens while preserving spatial-temporal features of a chunk? Motivated by Video-ChatGPT [1], we perform spatial-temporal pooling on the spatio-temporal features. Particularly, global spatial average pooling for each frame is performed and thus we obtain M tokens for the M frames (e.g., 4 tokens). Temporal pooling for each spatial position is performed to have $N = \bar{h} \times \bar{w} = 8 \times 8 = 64$ tokens. We have $N + M = 64 + 4 = 68$ tokens $\bar{F}_i^j \in \mathbb{R}^{(N+M) \times D}$, with D dimension for each token. Please see Supplementary for more details. Compared with the original 1024 in a chunk, the number of tokens has been reduced to 6.6%. We store the reduced chunk tokens in a memory to facilitate retrieval for the later LLM inference.

In contrast to Video-ChatGPT [1], which performs global spatial and temporal pooling over the entire video, ours with chunks is capable of *preserving local details* and is suited for long video reasoning.

B. Question-guided Retrieval for Chunk Selection

For a long video V_i with abundant video chunks, we retrieve and select the K most relevant chunks based on the question/query and use them as input to the LLM. The top K retrieval aims to efficiently identify the most informative video segments for answering the given question, reducing the memory and computational burden to LLM and excluding the interference from irrelevant content.

We encode the question Q_i into a feature vector $\mathbf{q}_i \in \mathbb{R}^D$ using the frozen CLIP text encoder f_θ and a learnable MLP block ψ as

$$\mathbf{q}_i = \psi(f_\theta(Q_i)), \quad (1)$$

where the MLP block is a two-layer perceptron consisting of two fully connected layers and an ReLU activation function in between. This MLP transformation strengthens the correlation between the question representation and the potential corresponding chunk features for chunk selection. The MLP block is very lightweight with negligible number of parameters (i.e., 1.8M), while facilitating the question-aware retrieval for long video understanding. Note that achieving this is non-trivial,

as we do not have any ground-truth locations of the question relevant chunks for supervision. The purpose of adding an MLP block to the text features is to enable learnable retrieval, i.e., the learnable selection of question-related video chunks. Another alternative design is to apply an MLP to the vision features during retrieval or apply MLPs to both. For a video question pair in inference, if we apply the MLP to the text encoder, we only need the inference through the MLP once. If we apply the MLP to the vision encoder, we need the inference through the MLP for every chunk. For simplicity, we only apply to the text feature.

To identify the question-related chunks, we measure the affinity between the question and the chunks. We define the similarity score between the question representation \mathbf{q}_i and the j^{th} chunk of video V_i as the average cosine similarity between \mathbf{q}_i and the $N + M$ chunk tokens as

$$s_i^j = \frac{1}{N + M} \sum_{n=1}^{N+M} \frac{\mathbf{q}_i \cdot \mathbf{u}_{i,n}^j}{\|\mathbf{q}_i\| \|\mathbf{u}_{i,n}^j\|}, \quad (2)$$

where $\mathbf{u}_{i,n}^j$ denotes the n^{th} token in the j^{th} chunk (of video V_i), $n = 1, \dots, N + M$. We rank the video chunks based on their similarity scores s_i^j (where $j = 1, \dots, L_i$) and select the top K most relevant chunks. The $K \times (N + M)$ visual tokens of these chunks are input to the LLM after a linear projection (a fully connected layer) on each token.

C. End-to-End Optimization

We train the network using an end-to-end optimization approach with the video instruction data. The image encoder, text encoder, and the LLM are frozen during the training. Only the parameters of the MLP block and projector are optimized. For a video-text pair, we introduce soft matching (SM) loss $\mathcal{L}_i^{\text{SM}}$ to regularize the similarity learning as

$$\mathcal{L}_i^{\text{SM}} = -\frac{\mathbf{q}_i \cdot \bar{\mathbf{v}}_i}{\|\mathbf{q}_i\| \|\bar{\mathbf{v}}_i\|}, \quad \text{where } \bar{\mathbf{v}}_i = \frac{\sum_{j=1}^{L_i} e^{s_i^j} \mathbf{v}_i^j}{\sum_{j=1}^{L_i} e^{s_i^j}}, \quad (3)$$

where $\bar{\mathbf{v}}_i$ is a weighted combination of the \mathcal{L}_i chunk features. For a weight $e^{s_i^j}$, e denotes the base of the natural logarithm, s_i^j denotes the similarity score between the query and the j^{th} chunk features (see Eq. (2)) of the video V_i . \mathbf{v}_i^j denotes the averaged token feature of the j^{th} chunk, i.e., $\mathbf{v}_i^j = \frac{1}{N+M} \sum_{n=1}^{N+M} \mathbf{u}_{i,n}^j$. The soft matching loss aims to align the aggregated visual feature with the question feature by adjusting weights. Through the optimization of the MLP block, high weights are assigned to video chunks closely related to the question and low weights to less relevant chunks, thus improving the selection of relevant chunks for accurate question answering.

The overall loss is

$$\mathcal{L}_i = \mathcal{L}_i^{\text{pred}} + \lambda \mathcal{L}_i^{\text{SM}}, \quad (4)$$

where $\mathcal{L}_i^{\text{pred}}$ denotes the cross-entropy loss between the generated prediction and groundtruth answer (a.k.a. LLM loss). λ is a hyper-parameter (we set to 10) that balances the contribution of the regularization term (see Table X for the ablation).

TABLE I: Information of the evaluation datasets, including the number of videos, the number of QA pairs, and the average video duration.

| Dataset | #Video | #QA | Duration (sec.) |
|----------------|--------|------|-----------------|
| Activitynet-QA | 800 | 8000 | 114 |
| EgoSchema | 5031 | 5031 | 180 |
| Next-QA | 570 | 4996 | 44 |
| IntentQA | 567 | 2134 | 47 |
| WildQA | 261 | 652 | 71 |
| QaEgo4D | 166 | 1854 | 495 |
| lifeQA | 49 | 372 | 74 |
| Social-IQ 2.0 | 144 | 876 | 60 |

IV. EXPERIMENTS

A. Implementation Details

Following Video-ChatGPT [1], we use LLaVA [17] as our base model. We utilize the pre-trained CLIP ViT-L/14 [20] as our image encoder and extract the feature from the second-to-last layer as the $h \times w$ visual tokens of a frame. We use the fine-tuned Vicuna (7B) from LLaVA as our LLM. For the text encoder, we use the pre-trained CLIP ViT-L/14 text encoder and extract the class token feature of the penultimate layer. Each of the two fully connected layers within the MLP block is equipped with 1024 neurons. The projector has 4096 neurons.

We only fine-tune the MLP block and the projector while keeping the image encoder, the text encoder and the LLM frozen. We fine-tune the model for 3 epochs using video instruction data, with a learning rate of 2e-5 and a batch size of 40. Training our model takes about 24h on an A100 80GB GPU. We set K to 5, resulting in $5 \times (64 + 4) = 340$ visual tokens as the input to the LLM. This is comparable to the number of visual tokens used in Video-ChatGPT (356 visual tokens).

For VideoChat-GPT, only the projector of 4.2M parameters is trained. In our framework, besides the projector, we added a small trainable MLP block of 1.8M parameters. Our total number of trainable parameters is 6.0M, which is very small considering the total model size is 6.7B.

B. Datasets and Evaluation

We use Video Instruction Data collected by Maaz *et al.* [1] for video instruction tuning. This dataset contains about 100k question and answer pairs based on the Activitynet-QA dataset (average duration 180 seconds), including various types of questions.

We evaluate the generalization (zero shot) performance of our framework on long video QA datasets Activitynet-QA [31], EgoSchema [32], NExt-QA [33], and IntentQA [34]. To widely evaluate the effectiveness of our model, besides the four popular datasets, we also tested on other long video QA datasets WildQA [35], QaEgo4D [36], lifeQA [37], and Social-IQ 2.0 [38]. Table I shows specific information about each dataset. We perform ablation studies on Activitynet-QA, WildQA, QaEgo4D, lifeQA, and Social-IQ 2.0. Note that the other widely used datasets MSVD-QA [39], MSRVTT-QA [40] for video QA are not suitable, which have average

TABLE II: Performance comparison with the state-of-the-art methods for video QA on Activitynet-QA.

| Model | Acc./Score |
|-------------------------|-----------------|
| Video-LLaMA [4] | 12.4/1.1 |
| FrozenBiLM [41] | 24.7/- |
| VideoChat [3] | 26.5/2.2 |
| LLaMA-Adapter [42] | 34.2/2.7 |
| Elysium [43] | 43.4/2.9 |
| Video-LLaVA [44] | 45.3/3.3 |
| MovieChat [25] | 45.7/3.1 |
| BT-Adapter [45] | 46.1/3.2 |
| Chat-UniVi [46] | 46.1/3.3 |
| MiniGPT4-video(7B) [47] | 46.3/- |
| LLaMA-VID(7B) [26] | 47.4/3.3 |
| Video-ChatGPT [1] | 47.8/3.3 |
| VideoChat2 [48] | 49.1/3.3 |
| R-VLM (Ours) | 49.7/3.3 |

TABLE III: Performance comparison with the state-of-the-art methods for video QA on EgoSchema fullset.

| Model | Acc. |
|---------------------|-------------|
| SeViLA [24] | 22.7 |
| FrozenBiLM [41] | 26.9 |
| mPLUG-Owl [22] | 31.1 |
| Intervideo [49] | 32.1 |
| TimeChat [50] | 33.0 |
| LLoVi [51] | 33.5 |
| Vamos(13B) [52] | 36.7 |
| R-VLM (Ours) | 40.2 |

duration of only 10 seconds and 15 seconds, being too short for evaluation.

We assess model performance using accuracy and a 0-5 similarity score, respectively, as per Video-ChatGPT [1], with ChatGPT (gpt-3.5-turbo) evaluating the correctness of predictions through binary and numerical judgments. See Supplementary Section A for more information.

C. Comparison with Other Models

We compare our final scheme *R-VLM* (Retrieval based video-language model) with the baseline method *Video-ChatGPT* [1] and the other state-of-the-art methods. We treat *Video-ChatGPT* as our baseline method, where we use the same training dataset, LLM of LLaMA-7B, and visual encoder CLIP-L as *Video-ChatGPT*.

Table II, III, IV, and Table V show the performance comparison on Activitynet-QA, EgoSchema, NExt-QA, and IntentQA, respectively. We can see that our model achieves the state-of-the-art performance. On Activitynet-QA, our *R-VLM* outperforms LLaMA-VID-7B by 2.3% in accuracy. Our *R-VLM* achieves competitive performance with VideoChat2, even though VideoChat2 uses much more training data than ours (1.1 million vs. our 100K video-text pairs).

On the WildQA, QaEgo4D, lifeQA, and Social-IQ 2.0 datasets, Table VI shows the comparison with the baseline method *Video-ChatGPT*, and the method of *Video-LLaMA* [23]. *R-VLM* outperforms *Video-ChatGPT* significantly by **6.8%**, **2.8%**, **4.8%**, **6.0%** in accuracy, respectively. Ours consistently achieves the best average score. Note that the number

TABLE IV: Performance comparison with the state-of-the-art methods for video QA on NExt-QA.

| Model | Des. | Tem. | Cau. | Acc. |
|-------------------|-------------|-------------|-------------|-------------|
| Just-Ask [53] | 36.0 | 31.8 | 30.4 | 38.4 |
| CLIP [20] | 57.0 | 38.1 | 43.6 | 43.9 |
| InternVideo [49] | 65.1 | 43.4 | 48.0 | 49.1 |
| Mistral(7B) [54] | - | - | - | 51.1 |
| VFC [55] | 64.1 | 45.4 | 51.6 | 51.5 |
| LLoVi(7B) [51] | 63.2 | 55.6 | 47.9 | 54.3 |
| MVU(13B) [56] | 64.1 | 55.4 | 48.1 | 55.2 |
| Video-ChatGPT [1] | 62.7 | 48.8 | 58.8 | 56.2 |
| R-VLM (Ours) | 63.1 | 52.0 | 59.9 | 58.7 |

TABLE V: Performance comparison with the state-of-the-art methods for video QA on IntentQA dataset.

| Model | Acc. |
|------------------|-------------|
| Random | 20.0 |
| HGQA [57] | 47.7 |
| VGT [58] | 51.3 |
| BlindGPT [59] | 51.6 |
| Mistral(7B) [54] | 50.4 |
| LLoVi(7B) [51] | 53.6 |
| CaVIR [34] | 57.6 |
| R-VLM (Ours) | 57.7 |

TABLE VI: Comparison with the other video-language models, including Video-LLaMA [23] and the baseline method Video-ChatGPT [1]. We report the accuracy (%)/ average score.

| Dataset | Video-LLaMA | Video-ChatGPT | R-VLM (Ours) |
|---------------|--------------------|---------------|-------------------|
| WildQA | 63.19/3.18 | 58.00/3.30 | 64.82/3.39 |
| QaEgo4D | 35.35 /1.94 | 29.74/2.43 | 32.51/2.45 |
| lifeQA | 35.75/2.32 | 33.87/2.55 | 38.71/2.61 |
| Social-IQ 2.0 | 55.78/2.90 | 57.73/3.26 | 63.65/3.40 |

of visual tokens of our *R-VLM* is comparable to that of *Video-ChatGPT* (*i.e.*, 340 vs. 356), making a fair comparison. This demonstrates the effectiveness of our learnable retrieval-based design, which facilitates the exploration of the most informative visual tokens and preservation of necessary vision details for QA. We found that when evaluating Video-LLaMA, the metric of accuracy is not as reliable as the score. *Video-LLaMA* is prone to give detailed description of the entire video, whereas the answer is usually not question-specific. The accuracy metric treats such answer as correct, while the score rating is relatively reasonable. Fig. 4 in Supplementary Material E shows a typical example on QaEgo4D, where the answer includes much irrelevant (or incorrect) information while the answer is submerged in the overall answer. In contrast, our model provides more concise and accurate answers. This explains why our accuracy is lower than Video-LLaMA on QaEgo4D.

D. Ablation Studies

In this section, we study and validate the effectiveness of our retrieval designs, the soft matching loss, chunk-wise design,

Sevilla [24] achieves an average accuracy of 73.8%, where the model is trained on NExt-QA. In contrast, our model has not seen Next-QA during training. VideoChat2 [48] achieves an average accuracy of 68.6%. It uses much more data for training (1.9M samples vs. ours using 100K).

the influence of hyperparameter K , and the influence of the time duration of a chunk, respectively.

Effectiveness of Retrieval for Chunk Selection Within our framework, we compare our retrieval mechanism and the uniform sampling strategy for the selection of $K = 5$ chunks as context input to the LLM. For the uniform sampling setting which we name as *R-VLM w/ Uni.*, the model selects K from N video chunks uniformly instead of based on question guided retrieval. Table VII shows that our final scheme *R-VLM* with learnable retrieval-based strategy outperforms *R-VLM w/ Uni.* by 3.6%, 0.9%, 2.2%, and 5.7% on WildQA, QaEgo4D, lifeQA, and Social-IQ 2.0, respectively. For a long video, the video chunks relevant to the question usually account for a small portion of the entire video. It is difficult to hit these question-related chunks with uniform sampling. A large language model may not correctly answer a question when it accepts video chunks not correlated with the question. In contrast, our learnable retrieval learns to select the chunks most relevant to the question, providing more reliable and less redundant information to the LLM for effective inference. Visualizations of the selected chunks in Fig. 2 also validate this and show that our retrieval-based model is interpretable, indicating from where and why the model produces the answer.

Effectiveness of Learnable Retrieval vs. Off-the-shelf CLIP based Retrieval We propose the learnable retrieval by introducing the MLP block. One may wonder the performance of using *off-the-shelf* CLIP class token features to match question and chunk features inside our framework. To answer this, we design a scheme *R-VLM w/ CLIP M.* for comparison. For a chunk, we use the averaged class token feature of the last layer of the CLIP image encoder as the vision chunk feature, and the class token feature of the last layer of the CLIP text encoder as the question feature for matching. There is no learnable parameters for the retrieval. Table VII shows that **our *R-VLM* with learnable retrieval consistently outperforms *R-VLM w/ CLIP M.*, upto 7.3% in accuracy** on the lifeQA dataset. That may be because the CLIP matching is originally designed for image and caption matching, which is not robust to the image and question matching. Thanks to the adaptation of the text encoder through a learnable MLP block, our question guided retrieval can better identify the relevant video chunks.

Influence of Soft Matching (SM) Loss In order to regularize the learning of the MLP block for better retrieval, we introduce SM loss. Table VII shows the comparison of our framework without the SM loss (*R-VLM w/o SM*) and that with SM loss (*R-VLM*). We can see that incorporating the SM loss significantly improves the performance. Our final scheme with the SM loss *i.e.*, *R-VLM* outperforms that without SM Loss. SM Loss uses the cosine similarity between text embedding and video tokens as weight to re-weight the video tokens to obtain new video tokens. Then maximize the similarity between the new video tokens and the text embedding. This facilitates our learnable retrieval layer to find the video clips most similar to the questions.

Influence of LLM Loss to Retrieval The instruction tuning

TABLE VII: Comparison of different methods and ablation studies. All these models are trained using the same video instruction data. *R-VLM* denotes our final scheme with learnable retrieval. *Video-ChatGPT* is our baseline method. *R-VLM w/ Uni.* denotes uniform sampling of K chunks in our framework instead of retrieval-based sampling. *R-VLM w/ CLIP M.* denotes that we use the final CLIP class token features of vision and text for matching in our framework, without incorporating learnable parameters for retrieval. *R-VLM w/o SM* denotes that we do not use the proposed soft matching (SM) loss. *R-VLM w/o G.* denotes that the gradient back-propagation from the LLM loss \mathcal{L}_i^{pred} to the learnable MLP block ψ is disabled. We report the accuracy (%) / average score.

| Dataset | Video-ChatGPT | R-VLM w/ Uni. | R-VLM w/ CLIP M. | R-VLM w/o SM | R-VLM w/o G. | R-VLM |
|----------------|--------------------|---------------|------------------|--------------|--------------|-------------------|
| ActivityNet-QA | 47.81/3.27 | 49.34/3.32 | 48.86/3.30 | 48.39/3.32 | 48.30/3.31 | 49.65/3.34 |
| WildQA | <u>58.00</u> /3.30 | 61.23/3.36 | 60.31/3.27 | 59.94/3.28 | 62.27/3.32 | 64.82/3.39 |
| QaEgo4D | 29.74/2.43 | 31.57/2.44 | 31.52/2.43 | 31.12/2.36 | 31.66/2.46 | 32.51/2.45 |
| lifeQA | 33.87/2.55 | 36.56/2.56 | 31.45/2.42 | 36.29/2.47 | 37.09/2.60 | 38.71/2.61 |
| Social-IQ 2.0 | 57.73/3.26 | 57.96/3.24 | 61.17/3.28 | 57.22/3.17 | 62.43/3.36 | 63.65/3.40 |

TABLE VIII: Ablation study on the influence of K , evaluated in terms of accuracy (%)/score. We use bold to mark the best performance and underline to mark the second-best performance.

| Dataset | Video-ChatGPT | Ours(K=1) | Ours(K=3) | Ours(K=5) | Ours(K=7) |
|----------------|--------------------|-------------------|-------------------|-------------------|-------------------|
| ActivityNet-QA | 47.81/3.27 | 46.75/3.27 | 48.10/3.31 | <u>49.65/3.34</u> | 49.76/3.34 |
| WildQA | <u>58.00</u> /3.30 | 57.45/3.18 | 60.58/3.31 | 64.82/3.39 | <u>63.44/3.39</u> |
| QaEgo4D | 29.74/2.43 | 32.42/2.41 | 32.04/2.42 | <u>32.51/2.45</u> | 32.81/2.42 |
| lifeQA | 33.87/2.55 | <u>37.63/2.62</u> | <u>38.44/2.62</u> | 38.71/2.61 | <u>37.63/2.65</u> |
| Social-IQ 2.0 | 57.73/3.26 | 63.92/3.44 | 60.89/3.34 | <u>63.65/3.40</u> | 62.89/3.34 |
| Average | 44.84/2.89 | 47.86/2.91 | 47.99/2.92 | 49.92/2.96 | <u>49.19/2.95</u> |

with the LLM loss (\mathcal{L}_i^{pred}) back-propagates the gradient also to the learnable MLP block ψ , which facilitates the selection of right chunks for retrieval. When we disable the back-propagation to ψ , we have scheme *R-VLM w/o G.*. As shown in Table VII, our final scheme *R-VLM* that allows the back-propagation obviously outperforms *R-VLM w/o G.* by 2.6%, 0.9%, 1.6%, and 1.2% on WildQA, QaEgo4D, lifeQA, and Social-IQ 2.0.

Effectiveness of Chunk-wise Design *Video-ChatGPT* performs video level spatial temporal pooling to obtain 356 visual tokens. Such global pooling would result in loss of details, especially when the question-related video segments take a small portion of the entire video. In our design, we perform chunk level spatial temporal pooling to preserve more information about each chunk. Table VII shows that when we uniformly sample the chunks to have 340 visual tokens, *R-VLM w/Uni* obviously outperforms *Video-ChatGPT*, demonstrating the effectiveness of our chunk-wise design.

Influence of Hyperparameter K In general, when K is too small, it may lead to a loss of information necessary to answer the question. When K is too large, interference may be introduced, confusing the LLM. Table VIII shows the results of using different K . We found that as K gradually increases from 1 to 5, the average performance increases. When K increases from 5 to 7, the performance decreases. We found $K = 5$ presents a good trade-off on most datasets, even though there are slight differences on different datasets. We leave the adaptive design of K as future work.

Influence of the Time Duration of a Chunk In considering the memory limitation and video redundancy, we sample at a low frame rate (1 fps). To allow a chunk to contain dynamic temporal information, we use 4 seconds that are expected to contain temporal dynamics as the chunk unit.

TABLE IX: Influence of the time duration of a chunk, evaluated in terms of accuracy (%)/score. 8f/c denotes 8frames/chunk.

| | Video-ChatGPT | R-VLM(8f/c) | R-VLM(4f/c) |
|----------------|---------------|-------------|-------------------|
| ActivityNet-QA | 47.81/3.27 | 49.24/3.31 | 49.65/3.34 |
| WildQA | 58.00/3.30 | 62.58/3.37 | 64.82/3.39 |
| QaEgo4D | 29.74/2.43 | 32.36/2.43 | 32.51/2.45 |
| lifeQA | 33.87/2.55 | 36.83/2.63 | 38.71/2.61 |
| Social-IQ 2.0 | 57.73/3.26 | 62.20/3.33 | 63.65/3.40 |

We study the influence of the time duration of a chunk by comparing the use of 4 frames (4 seconds) and 8 frames (8 seconds) as a chunk at the same sample rate of 1 fps. Table IX shows the performance comparison. We can see that the performance of using 4 frames/chunk is better than that using 8 frames/chunk. Firstly, 4 frames/chunk allows identification of shorter temporal segments. Secondly, it preserves more spatial details than 8 seconds per chunk since an 8-second chunk pools features over a longer period. Both the two settings outperform the baseline method *Video-ChatGPT*.

Influence of the Hyperparameter λ We determine λ based on our previous experiences, where we usually can obtain satisfactory results by setting different losses at the same magnitude. This is a simple way to ensure that different losses are considered in optimization. We found when we set λ as 10, the two loss terms are at the similar magnitude. We also conducted ablation study on the choose of λ by setting it to 1, 10, and 100. Table X shows the comparison. We can see that $\lambda = 10$ provides the best performance on average, slightly better than that of $\lambda = 1$.

E. Visualization Analysis

We visualize an example from QAEgo4D in Fig. 2. More examples from QAEgo4D and WildQA are in Fig. 4, Fig. 5

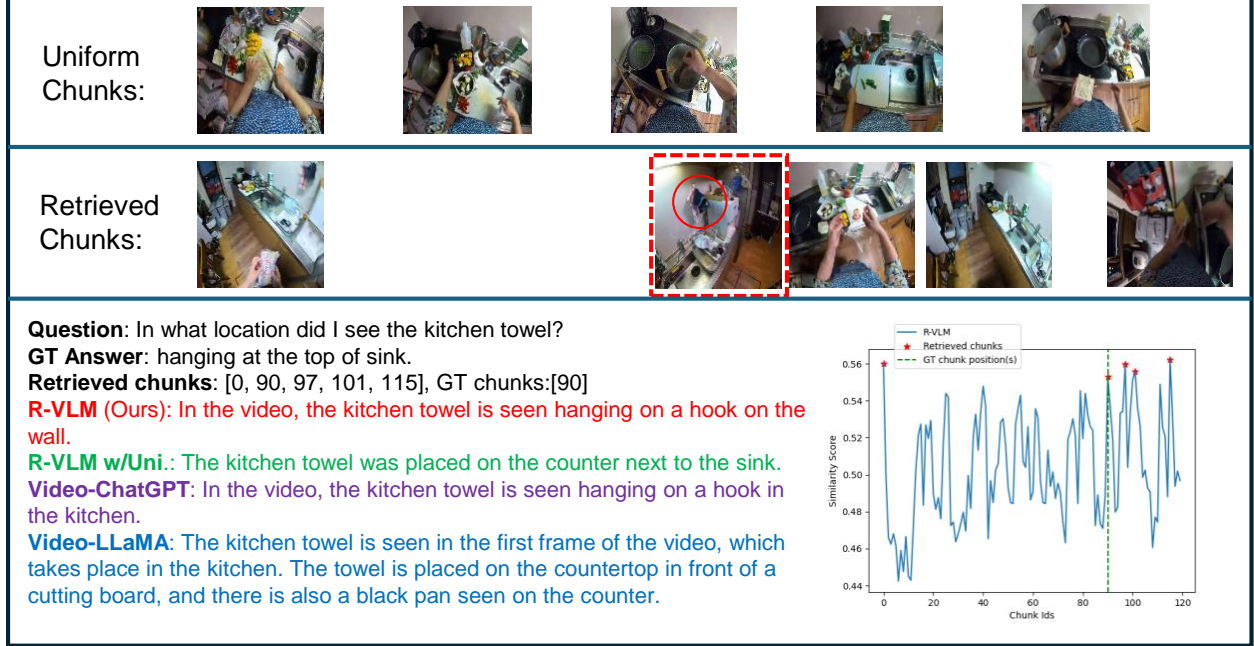


Fig. 2: Visualization of video QA examples from QAEgo4D. The kitchen towel related to the question does not appear in the uniformly sampled video chunks. The second chunk selected by our model contains kitchen towel. Our answer states that the towel is hanging on a hook on the wall. Video-LLaMA answers incorrectly, where the towel does not appear in the first frame of the video, and it is not be placed on the countertop in front of a cutting board. Note that we use a sampled frame in a chunk to illustrate the chunk in the first two rows.

TABLE X: Ablation study on λ .

| | $\lambda=1$ | $\lambda=10$ | $\lambda=100$ |
|----------------|----------------------------|----------------------------|--------------------|
| ActivityNet-QA | 49.70 /3.32 | 49.65/ 3.34 | 49.06/3.33 |
| WildQA | 64.42/ 3.41 | 64.82 /3.39 | 63.34/3.35 |
| QaEgo4D | 34.57 / 2.50 | 32.51/2.45 | 32.85/2.48 |
| lifeQA | 36.49/2.56 | 38.71 /2.61 | 36.93/ 2.67 |
| Social_IQ 2.0 | 62.77/3.38 | 63.65 / 3.40 | 60.71/3.32 |
| Average | 49.59/3.03 | 49.87 / 3.04 | 48.58/3.03 |

in Supplementary Material E, with the following information.

1) The first row shows the video chunk examples by uniformly selecting 5 video chunks. 2) The second row shows the retrieved 5 chunks (arranged in chronological order) in our *R-VLM*. We mark the groundtruth chunks by red box. 3) We show the curve of the learned similarity score (see Eq. (2)) based on which the top K chunks are selected. The horizontal axis represents the indices of chunks and the vertical axis denotes the similarity score. The groundtruth chunks and our retrieved chunks are also marked. 4) The question and answers from different models.

We can see that the predicted answers of our *R-VLM* is more accurate than *Video-ChatGPT*, and *Video-LLaMA*. For QAEgo4D, the average duration is about 8 minutes (120 video chunks), whereas the groundtruth segments span only 2% of the entire video on average. It is difficult to hit groundtruth video segments by uniformly sampling $K (= 5)$ chunks among 120 video chunks. Fig. 2 shows that the fragments selected by uniform sampling are in general irrelevant to the problem. Our learnable retrieval can accurately find the segments where the

TABLE XI: Average time cost for 60 seconds videos from Social-IQ 2.0. The first part is feature extraction and the second part is retrieval and LLM inference.

| | Feature Extraction | Retrieval & LLM inference | Total |
|----------------|--------------------|---------------------------|-------|
| Time (seconds) | 0.14 | 2.42 | 2.56 |

answer lies in. Feeding the correct chunks to the LLM makes it possible to obtain the correct answer to the question.

Besides the successful cases, we present some failed cases in Fig. 9 of Supplementary Material E. There are two main cases of failure. One is that the retrieval did not select the correct video chunks. The other is that the retrieval correctly identified the correct video chunks, but the answer was wrong. For the latter cases, we think more powerful vision feature extractor and LLMs would alleviate the problem.

F. Computational Complexity

The computational cost of our framework mainly comes from two parts. The first part is to encode the video frames through the CLIP encoder and the spatial-temporal pooling to get chunks. The second part is the retrieval of $K = 5$ chunks and put them to the LLM for inference.

On a single A100, we tested 120 videos with 60 seconds each from Social-IQ 2.0 and calculated the average inference time for a video, as shown in Table XI. For a video, the first part for vision feature extraction takes an average of 0.14 seconds (in parallel for 60 frames), and the second part (mainly LLM inference) takes an average of 2.42 seconds.

TABLE XII: Analysis of FLOPs saving of our scheme for LLM inference. *Avg.chunks* denotes the average number of video chunks. S_{vis} denotes the average number of visual tokens of all the chunks of a video (obtained by multiplying *Avg.Chunks* by the number of visual tokens per chunk (*i.e.*, 68)). S'_{vis} denotes the average number of visual tokens of the selected $K = 5$ chunks of a video ($5 \times 68 = 340$).

| | WildQA | QaEgo4D | lifeQA | Social-IQ 2.0 |
|--------------------|--------|---------|--------|---------------|
| <i>Avg. chunks</i> | 19 | 122 | 20 | 16 |
| S_{vis} | 1292 | 8296 | 1360 | 1088 |
| S'_{vis} | 340 | 340 | 340 | 340 |
| <i>Save</i> | 69% | 95% | 71% | 64% |

The total time is 2.56 seconds. The retrieval by encoding the question representation, and calculating the similarity scores between the question representation and the chunks, is very fast with almost negligible time. Note that for a longer video, the time consumption for LLM inference does not increase since the input number of visual tokens to the LLM is fixed (*i.e.*, $68 \times 5 = 340$) in our scheme, which is favored for long video or streaming video understanding.

The FLOPs for LLM inference can be roughly estimated as $2PS$, where P denotes the number of parameters, and S denotes the number of tokens. The computational complexity of LLM is proportional to the number of tokens which consists of text tokens (question and answer) and visual tokens. The LLM model size P is 6.7B. On the training dataset, the average number of tokens for question and answers is 80, *i.e.*, $S_{tex} = 80$. This varies on different testing datasets. For simplicity, we assume the number is the same for all the datasets. We denote the number of visual tokens as S_{vis} . The total number of tokens is then $S = S_{tex} + S_{vis}$. The saved computational cost (FLOPs) for LLM inference can be computed approximately as

$$FLOPs_Saved = \frac{S_{vis} - S'_{vis}}{S_{tex} + S_{vis}}. \quad (5)$$

We show the computation saving of four long video datasets in Table 5. **Thanks to our retrieval, only $K = 5$ chunks ($S'_{vis} = 5 \times 68 = 340$ tokens) instead of all the chunks are needed as the input to LLM. The saved computational cost (FLOPs) ranges from 69% to 95%, demonstrating the high efficiency of our solution.**

Moreover, our retrieval-based solution can significantly save the memory consumption. For an A100 GPU of 80G memory, given extracted chunk features, when we set batch size to 40 and K to 5, the memory occupation is about 70G in training. In contrast, when a baseline scheme without using retrieval that all the chunks (instead of 5 selected chunks) are input to LLM, videos longer than 40 seconds are not able to be filled to the memory (out of memory) in training. In contrast, our scheme could support very long videos (even 80+ hours).

V. CONCLUSION

The comprehension of long videos using LLMs remains an under-explored area. There are two main challenges associated

<https://medium.com/@dzmitrybahdanau/the-flops-calculus-of-language-model-training-3b19c1f025e4>

with comprehending long videos. 1) Long videos generally lead to abundant visual tokens, which increase computational cost for LLM inference. 2) Global aggregation of visual tokens inevitably results in the loss of vision details especially when the question relevant video chunks take only a small portion of the entire video. Moreover, question irrelevant chunks introduce interference. In this work, we address these issues by introducing a simple yet effective retrieval-based video-language model (R-VLM) for long-video understanding. Our R-VLM effectively reduces the number of video tokens, preserves the most informative information, eliminates noise interference, and thus enhances system performance. Our experimental results demonstrate the effectiveness of our designs for comprehending long videos.

REFERENCES

- [1] M. Maaz, H. Rasheed, S. Khan, and F. S. Khan, “Video-ChatGPT: Towards detailed video understanding via large vision and language models,” *arXiv preprint arXiv:2306.05424*, 2023.
- [2] J. Wang, D. Chen, C. Luo, X. Dai, L. Yuan, Z. Wu, and Y.-G. Jiang, “Chatvideo: A tracklet-centric multimodal and versatile video understanding system,” *arXiv preprint arXiv:2304.14407*, 2023.
- [3] K. Li, Y. He, Y. Wang, Y. Li, W. Wang, P. Luo, Y. Wang, L. Wang, and Y. Qiao, “Videochat: Chat-centric video understanding,” *arXiv preprint arXiv:2305.06355*, 2023.
- [4] H. Zhang, X. Li, and L. Bing, “Video-LLaMA: An instruction-tuned audio-visual language model for video understanding,” *arXiv preprint arXiv:2306.02858*, 2023.
- [5] R. F. Thompson and S. A. Madigan, *Memory: the key to consciousness*. Princeton University Press, 2013, vol. 3.
- [6] Z. Yuan, S. Sun, L. Duan, C. Li, X. Wu, and C. Xu, “Adversarial multimodal network for movie story question answering,” *IEEE Transactions on Multimedia*, vol. 23, pp. 1744–1756, 2020.
- [7] W. Zhang, S. Tang, Y. Cao, S. Pu, F. Wu, and Y. Zhuang, “Frame augmented alternating attention network for video question answering,” *IEEE Transactions on Multimedia*, vol. 22, no. 4, pp. 1032–1041, 2020.
- [8] J. Wang, B.-K. Bao, and C. Xu, “Dualvgr: A dual-visual graph reasoning unit for video question answering,” *IEEE Transactions on Multimedia*, vol. 24, pp. 3369–3380, 2021.
- [9] T. Qian, R. Cui, J. Chen, P. Peng, X. Guo, and Y.-G. Jiang, “Locate before answering: Answer guided question localization for video question answering,” *IEEE Transactions on Multimedia*, 2023.
- [10] F. Zhang, R. Wang, F. Zhou, Y. Luo, and J. Li, “Psam: Parameter-free spatiotemporal attention mechanism for video question answering,” *IEEE Transactions on Multimedia*, 2023.
- [11] Z. Guo, J. Zhao, L. Jiao, X. Liu, and F. Liu, “A universal quaternion hypergraph network for multimodal video question answering,” *IEEE Transactions on Multimedia*, vol. 25, pp. 38–49, 2021.
- [12] Y. Cheng, H. Fan, D. Lin, Y. Sun, M. Kankanhalli, and J.-H. Lim, “Keyword-aware relative spatio-temporal graph networks for video question answering,” *IEEE Transactions on Multimedia*, 2023.
- [13] J. Jiang, Z. Liu, and N. Zheng, “Livlr: A lightweight visual-linguistic reasoning framework for video question answering,” *IEEE Transactions on Multimedia*, vol. 25, pp. 5002–5013, 2022.
- [14] J.-B. Alayrac, J. Donahue, P. Luc, A. Miech, I. Barr, Y. Hasson, K. Lenc, A. Mensch, K. Millican, M. Reynolds *et al.*, “Flamingo: a visual language model for few-shot learning,” *Advances in Neural Information Processing Systems*, vol. 35, pp. 23716–23736, 2022.
- [15] J. Li, D. Li, S. Savarese, and S. Hoi, “Blip-2: Bootstrapping language-image pre-training with frozen image encoders and large language models,” *arXiv preprint arXiv:2301.12597*, 2023.
- [16] D. Zhu, J. Chen, X. Shen, X. Li, and M. Elhoseiny, “Minigpt-4: Enhancing vision-language understanding with advanced large language models,” *arXiv preprint arXiv:2304.10592*, 2023.
- [17] H. Liu, C. Li, Q. Wu, and Y. J. Lee, “Visual instruction tuning,” *Advances in Neural Information Processing Systems*, 2023.

This paper is the result of an open source research project starting from 2023.

[18] S. Huang, L. Dong, W. Wang, Y. Hao, S. Singhal, S. Ma, T. Lv, L. Cui, O. K. Mohammed, Q. Liu *et al.*, “Language is not all you need: Aligning perception with language models,” *arXiv preprint arXiv:2302.14045*, 2023.

[19] D. Surís, S. Menon, and C. Vondrick, “Vipergpt: Visual inference via python execution for reasoning,” in *Proceedings of the IEEE/CVF International Conference on Computer Vision*, 2023, pp. 11 888–11 898.

[20] A. Radford, J. W. Kim, C. Hallacy, A. Ramesh, G. Goh, S. Agarwal, G. Sastry, A. Askell, P. Mishkin, J. Clark *et al.*, “Learning transferable visual models from natural language supervision,” in *International conference on machine learning*. PMLR, 2021, pp. 8748–8763.

[21] W. Dai, J. Li, D. Li, A. Tiong, J. Zhao, W. Wang, B. Li, P. Fung, and S. Hoi, “Instructblip: Towards general-purpose vision-language models with instruction tuning,” *Advances in Neural Information Processing Systems*, 2023.

[22] Q. Ye, H. Xu, G. Xu, J. Ye, M. Yan, Y. Zhou, J. Wang, A. Hu, P. Shi, Y. Shi *et al.*, “mplug-owl: Modularization empowers large language models with multimodality,” *arXiv preprint arXiv:2304.14178*, 2023.

[23] H. Zhang, X. Li, and L. Bing, “Video-LLaMA: An instruction-tuned audio-visual language model for video understanding,” *arXiv preprint arXiv:2306.02858*, 2023.

[24] S. Yu, J. Cho, P. Yadav, and M. Bansal, “Self-chained image-language model for video localization and question answering,” *Advances in Neural Information Processing Systems*, vol. 36, 2024.

[25] E. Song, W. Chai, G. Wang, Y. Zhang, H. Zhou, F. Wu, H. Chi, X. Guo, T. Ye, Y. Zhang *et al.*, “Moviechat: From dense token to sparse memory for long video understanding,” in *Proceedings of the IEEE/CVF Conference on Computer Vision and Pattern Recognition*, 2024, pp. 18 221–18 232.

[26] Y. Li, C. Wang, and J. Jia, “Llama-vid: An image is worth 2 tokens in large language models,” in *European Conference on Computer Vision*, 2024.

[27] S. Kim, J.-H. Kim, J. Lee, and M. Seo, “Semi-parametric video-grounded text generation,” *arXiv preprint arXiv:2301.11507*, 2023.

[28] M. C. Lin and S. Yang, “Vila: Efficient video-language alignment for video question answering,” in *European Conference on Computer Vision*. Springer, 2024.

[29] H. Wang, C. Lai, Y. Sun, and W. Ge, “Weakly supervised gaussian contrastive grounding with large multimodal models for video question answering,” in *Proceedings of the 32nd ACM International Conference on Multimedia*, 2024, pp. 5289–5298.

[30] Z. Wang, S. Yu, E. Stengel-Eskin, J. Yoon, F. Cheng, G. Bertasius, and M. Bansal, “Videotree: Adaptive tree-based video representation for llm reasoning on long videos,” *arXiv preprint arXiv:2405.19209*, 2024.

[31] F. Caba Heilbron, V. Escorcia, B. Ghanem, and J. Carlos Niebles, “Activitynet: A large-scale video benchmark for human activity understanding,” in *Proceedings of the IEEE Conference on Computer Vision and Pattern Recognition*, 2015, pp. 961–970.

[32] K. Mangalam, R. Akshulakov, and J. Malik, “Egoschema: A diagnostic benchmark for very long-form video language understanding,” *Advances in Neural Information Processing Systems*, vol. 36, 2024.

[33] J. Xiao, X. Shang, A. Yao, and T.-S. Chua, “Next-qa: Next phase of question-answering to explaining temporal actions,” in *Proceedings of the IEEE/CVF conference on computer vision and pattern recognition*, 2021, pp. 9777–9786.

[34] J. Li, P. Wei, W. Han, and L. Fan, “Intentqa: Context-aware video intent reasoning,” in *Proceedings of the IEEE/CVF International Conference on Computer Vision*, 2023, pp. 11 963–11 974.

[35] S. Castro, N. Deng, P. Huang, M. G. Burzo, and R. Mihalcea, “In-the-wild video question answering,” in *International Conference on Computational Linguistics*, 2022, pp. 5613–5635.

[36] L. Bärmann and A. Waibel, “Where did i leave my keys? - episodic-memory-based question answering on egocentric videos,” in *Proceedings of the IEEE/CVF Conference on Computer Vision and Pattern Recognition (CVPR) Workshops*, June 2022, pp. 1560–1568.

[37] S. Castro, M. Azab, J. Stroud, C. Noujaim, R. Wang, J. Deng, and R. Mihalcea, “LifeQA: A real-life dataset for video question answering,” in *Proceedings of the Twelfth Language Resources and Evaluation Conference*, 2020, pp. 4352–4358.

[38] A. Wilf, L. Mathur, S. Mathew, C. Ko, Y. Kebe, P. P. Liang, and L.-P. Morency, “Social-iq 2.0 challenge: Benchmarking multimodal social understanding.” <https://github.com/abwilf/Social-IQ-2.0-Challenge>, 2023.

[39] D. Chen and W. B. Dolan, “Collecting highly parallel data for paraphrase evaluation,” in *Proceedings of the 49th Annual Meeting of the Association for Computational Linguistics: Human Language Technologies*, 2011, pp. 190–200.

[40] J. Xu, T. Mei, T. Yao, and Y. Rui, “Msr-vtt: A large video description dataset for bridging video and language,” in *Proceedings of the IEEE Conference on Computer Vision and Pattern Recognition*, 2016, pp. 5288–5296.

[41] A. Yang, A. Miech, J. Sivic, I. Laptev, and C. Schmid, “Zero-shot video question answering via frozen bidirectional language models,” *Advances in Neural Information Processing Systems*, vol. 35, pp. 124–141, 2022.

[42] P. Gao, J. Han, R. Zhang, Z. Lin, S. Geng, A. Zhou, W. Zhang, P. Lu, C. He, X. Yue *et al.*, “Llama-adapter v2: Parameter-efficient visual instruction model,” *arXiv preprint arXiv:2304.15010*, 2023.

[43] H. Wang, Y. Wang, Y. Ye, Y. Nie, and C. Huang, “Elysium: Exploring object-level perception in videos via mllm,” *arXiv preprint arXiv:2403.16558*, 2024.

[44] B. Lin, B. Zhu, Y. Ye, M. Ning, P. Jin, and L. Yuan, “Video-llava: Learning united visual representation by alignment before projection,” *arXiv preprint arXiv:2311.10122*, 2023.

[45] R. Liu, C. Li, Y. Ge, T. H. Li, Y. Shan, and G. Li, “Bt-adapter: Video conversation is feasible without video instruction tuning,” in *Proceedings of the IEEE/CVF Conference on Computer Vision and Pattern Recognition*, 2024, pp. 13 658–13 667.

[46] P. Jin, R. Takanobu, W. Zhang, X. Cao, and L. Yuan, “Chat-univ: Unified visual representation empowers large language models with image and video understanding,” in *Proceedings of the IEEE/CVF Conference on Computer Vision and Pattern Recognition*, 2024, pp. 13 700–13 710.

[47] K. Ataallah, X. Shen, E. Abdelrahman, E. Sleiman, D. Zhu, J. Ding, and M. Elhoseiny, “Minigpt4-video: Advancing multimodal llms for video understanding with interleaved visual-textual tokens,” *arXiv preprint arXiv:2404.03413*, 2024.

[48] K. Li, Y. Wang, Y. He, Y. Li, Y. Wang, Y. Liu, Z. Wang, J. Xu, G. Chen, P. Luo *et al.*, “Mvbench: A comprehensive multi-modal video understanding benchmark,” in *Proceedings of the IEEE/CVF Conference on Computer Vision and Pattern Recognition*, 2024, pp. 22 195–22 206.

[49] Y. Wang, K. Li, Y. Li, Y. He, B. Huang, Z. Zhao, H. Zhang, J. Xu, Y. Liu, Z. Wang *et al.*, “Internvideo: General video foundation models via generative and discriminative learning,” *arXiv preprint arXiv:2212.03191*, 2022.

[50] S. Ren, L. Yao, S. Li, X. Sun, and L. Hou, “Timechat: A time-sensitive multimodal large language model for long video understanding,” in *Proceedings of the IEEE/CVF Conference on Computer Vision and Pattern Recognition*, 2024, pp. 14 313–14 323.

[51] C. Zhang, T. Lu, M. M. Islam, Z. Wang, S. Yu, M. Bansal, and G. Bertasius, “A simple llm framework for long-range video question-answering,” *arXiv preprint arXiv:2312.17235*, 2023.

[52] S. Wang, Q. Zhao, M. Q. Do, N. Agarwal, K. Lee, and C. Sun, “Vamos: Versatile action models for video understanding,” *arXiv preprint arXiv:2311.13627*, 2023.

[53] A. Yang, A. Miech, J. Sivic, I. Laptev, and C. Schmid, “Just ask: Learning to answer questions from millions of narrated videos,” in *Proceedings of the IEEE/CVF international conference on computer vision*, 2021, pp. 1686–1697.

[54] A. Q. Jiang, A. Sablayrolles, A. Mensch, C. Bamford, D. S. Chaplot, D. d. I. Casas, F. Bressand, G. Lengyel, G. Lample, L. Saulnier *et al.*, “Mistral 7b,” *arXiv preprint arXiv:2310.06825*, 2023.

[55] L. Momeni, M. Caron, A. Nagrani, A. Zisserman, and C. Schmid, “Verbs in action: Improving verb understanding in video-language models,” in *Proceedings of the IEEE/CVF International Conference on Computer Vision*, 2023, pp. 15 579–15 591.

[56] K. Ranasinghe, X. Li, K. Kahatapitiya, and M. S. Ryoo, “Understanding long videos in one multimodal language model pass,” *arXiv preprint arXiv:2403.16998*, 2024.

[57] J. Xiao, A. Yao, Z. Liu, Y. Li, W. Ji, and T.-S. Chua, “Video as conditional graph hierarchy for multi-granular question answering,” in *Proceedings of the AAAI Conference on Artificial Intelligence*, vol. 36, no. 3, 2022, pp. 2804–2812.

[58] J. Xiao, P. Zhou, T.-S. Chua, and S. Yan, “Video graph transformer for video question answering,” 2022. [Online]. Available: <https://arxiv.org/abs/2207.05342>

[59] L. Ouyang, J. Wu, X. Jiang, D. Almeida, C. Wainwright, P. Mishkin, C. Zhang, S. Agarwal, K. Slama, A. Ray *et al.*, “Training language models to follow instructions with human feedback,” *Advances in Neural Information Processing Systems*, vol. 35, pp. 27 730–27 744, 2022.

APPENDIX

To better illustrate the procedure of visual token extraction of a chunk, Fig. 3 illustrates the spatial and temporal pooling for obtain 68 visual tokens for a chunk.

A. More Details on Evaluation Metrics

In this paper, we follow the metrics of accuracy and average score as proposed by Video-ChatGPT [1] for performance evaluation, where we use ChatGPT (gpt-3.5-turbo) to assist in judging the correctness of model predictions. ChatGPT accepts questions, groundtruth answers, and the model predictions as input. For each question-answer pair, ChatGPT gives a binary judgment of “yes” or “no” to identify whether the predicted answer is correct or not, for accuracy evaluation. Moreover, an integer score of 0-5 is also given by ChatGPT to indicate how similar the prediction is to the answer. 0 represents the lowest score and 5 represents the highest score.

B. Human Evaluation Results

We have conducted human studies in 100 samples of four test datasets on two models, the baseline scheme Video-ChatGPT, and our scheme R-VLM. We asked three people to blindly rate correct/wrong and scores and show the average evaluation results in Table R1-1. We can see that our method R-VLM achieves higher accuracy and score than Video-ChatGPT under human evaluation. The main trends from ChatGPT evaluation are consistent with our human evaluation but the values and relative gains between two schemes are different, which also indicates ChatGPT evaluation has a certain degree of reliability but are not perfect.

TABLE XIII: The results of human evaluation and ChatGPT evaluation on 100 samples, which are randomly selected from four test datasets.

| Evaluator | Video-ChatGPT | R-VLM (Ours) |
|-----------|---------------|--------------|
| ChatGPT | 48/2.98 | 50/3.03 |
| Human | 42.33/2.26 | 46.33/2.41 |

C. More Ablation Studies

Comparison with Q-Former-based Designs We compare our retrieval-based design with Q-former designs under our framework. 1) We use a Q-Former to globally aggregate all the chunk tokens to be the input of the LLM, where the input to Q-Former is the $L_i \times (N + M)$ tokens, where L_i denotes the number of chunks, $N + M = 68$ denotes the reduced number of tokens (through spatial-temporal pooling) in a chunk. The output is 340 visual tokens. There is no retrieval in this scheme, and we dub it VLM-QFormer. Table XIV shows the comparison with our scheme. We can see that our R-VLM outperforms VLM-QFormer significantly, thanks to the retrieval-based design which can exclude the inference of irrelevant visual tokens. 2) Similar to InstructBLIP [21], we use instruction-aware Q-Former to globally aggregate all the chunk tokens to be the input of the LLM. The difference with VLM-QFormer is that the instruction is also taken as the

input to Q-Former to learn instruction (question)-aware visual tokens. We dub this scheme as *VLM-InstructQFormer*. We can see that *VLM-InstructQFormer* outperforms *VLM-QFormer* on most datasets but is inferior to our *R-VLM*, demonstrating the effectiveness of our retrieval-based design for extracting question-relevant visual features.

TABLE XIV: Comparison with Q-Former based two designs under our framework, evaluated in terms of accuracy (%)/score.

| | VLM-Qformer | VLM-InstructQformer | R-VLM (Ours) |
|----------------|--------------------|---------------------|----------------------------|
| ActivityNet-QA | 49.34/ 3.35 | 48.94/3.33 | 49.65 /3.34 |
| WildQA | 58.59/3.16 | 58.28/3.17 | 64.82 / 3.39 |
| QaEgo4D | 30.58/2.35 | 31.23/2.41 | 32.51 / 2.45 |
| lifeQA | 35.48/2.56 | 37.10/ 2.62 | 38.71 /2.61 |
| Social-IQ 2.0 | 54.30/3.14 | 57.62/3.19 | 63.65 / 3.40 |

D. More Results on Other Datasets

We also report the results on the subset of EgoSchema in Table XV. It can be seen that our R-VLM method achieves the best performance.

E. More Visualization Results

We visualize more examples from the QAEgo4D and WildQA datasets in Fig. 4, Fig. 5 with the following information.

1) The first row shows the video chunk examples by uniformly selecting 5 video chunks. 2) The second row shows the retrieved 5 chunks (arranged in chronological order) in our *R-VLM*. We mark the groundtruth chunks by red box. 3) We show the curve of the learned similarity score (see Eq. (2)) based on which the top K chunks are selected. The horizontal axis represents the indices of chunks and the vertical axis denotes the similarity score. The groundtruth chunks and our retrieved chunks are also marked. 4) The question and answers from different models.

For the WildQA dataset, groundtruth segments usually locate at different locations in the video and last for a period of time. Although uniform sampling sometimes hits a certain groundtruth segments, there is no guarantee. In contrast, our learned retrieval can correctly hit the segments where the groundtruth segments are located on. In this way, the LLM can better understand the video and answer some detailed questions (refer to “vegetation types” in Fig. 5).

In addition to successful cases, we present some failed cases in Fig.9 of Appendix E. There are two main cases of failure. One is that the retrieval did not select the correct video chunks. The other is that the retrieval correctly identified the correct video chunks, but the answer was wrong. For the latter cases, we think more powerful vision feature extractor and LLMs would alleviate the problem.

F. More Discussion on Memory Cost

We have also estimated the memory cost for training different schemes when we set the batch size as 20 and use input video sequences of 80 seconds. Our scheme with $K=5$ uses similar size of memory (45.3 GB) as VideoChat-GPT (42.2

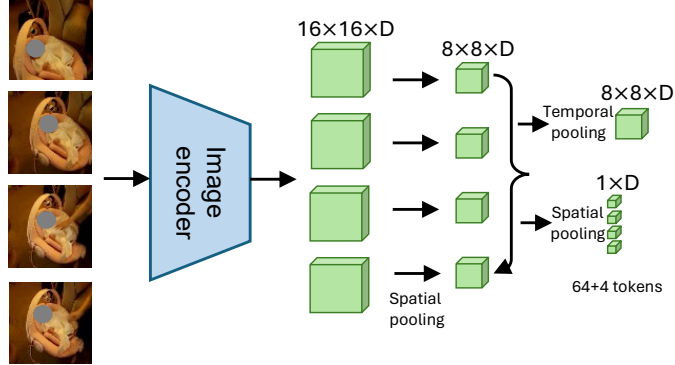


Fig. 3: Illustration of the spatial and temporal pooling to obtain 68 visual tokens for a chunk. We perform spatial average pooling with stride 2 to have $M \times \bar{h} \times \bar{w} = 4 \times 8 \times 8 = 256$ tokens per chunk, where $\bar{h} = h/2$ and $\bar{w} = w/2$. This is equivalent to taking the CLIP features of reduced resolution as the extracted feature. Global spatial average pooling for each frame is performed and thus we obtain M tokens for the M frames ($M = 4$). Temporal pooling for each spatial position is performed to have $N = \bar{h} \times \bar{w} = 8 \times 8 = 64$ tokens. Therefore, we have $N + M = 64 + 4 = 68$ tokens for a chunk.

TABLE XV: Performance comparison with the state-of-the-art methods for video QA on the EgoSchema subset of 500 testing pairs.

| Model | Acc. |
|---------------------|-------------|
| ViperGPT [19] | 15.8 |
| Video-ChatGPT [1] | 20.0 |
| SeViLA [24] | 25.7 |
| mPLUG-Owl [22] | 33.8 |
| Video-LLaVA [44] | 36.8 |
| R-VLM (Ours) | 46.0 |

GB). In contrast, the total memory cost without using retrieval (input all the chunks, in total 1360 visual tokens) is 75.1GB, demonstrating that our retrieval-based design (45.3GB) can significantly save memory and is efficient.

G. Discussion on the Effectiveness of Retrieval

There are no ground-truth locations of the question relevant chunks for supervision. The effectiveness of our learned chunk selection (retrieval) benefits from four aspects that promote the question (text) and vision alignment. First, the use of pretrained CLIP vision encoder and CLIP text encoder, where their features are trained to be matched/aligned. Second, the learnable MLP block (which follows the CLIP text encoder) makes it possible for the *question* and vision alignment, which the original CLIP pretraining (*caption* and vision alignment) has not been. As shown in Table VII in our main manuscript, *R-VLM w/ CLIP M.* denotes the use of the final CLIP class token feature of vision and text for matching instead of learnable retrieval. We can see that our final scheme *R-VLM* with learnable matching outperforms *R-VLM w/ CLIP M.* significantly. Third, the proposed soft matching (SM) loss promotes the alignment of question and vision features. *R-VLM w/o SM* denotes the scheme without using SM loss, which is inferior to *R-VLM*. Forth, the end-to-end instruction tuning (loss from the LLM) facilitates the selection of right chunks through the gradient back-propagation. Intuitively, only when the chunks are selected correctly, does the model generate the right answers. *R-VLM w/o G.* denotes our scheme but without

back-propagating the gradient from the LLM loss. *R-VLM* that allows such back-propagation to the learnable MLP block outperforms *R-VLM w/o G.* obvious. We can see that all these factors jointly make the retrieval-based solution feasible and efficient.

We have explored the retrieval-based solution for the long video understanding. We experimentally found that using $K = 5$ selected chunks can generate superior performance. Sample adaptive K should deliver optimal results but we leave this as future work.

When the retrieval does not select the correct video chunks, our model will fail to generate correct answers as some failed cases in Fig.9 (b) and (c). As a remedy, we could incorporate some global video tokens (e.g., like Video-ChatGPT) to assure the preservation of global information to alleviate this. We leave this as future work.

This paper presents work that aims to advance the field of video-language modeling. Our research is designed to be a positive force for innovation purpose. However, future applications should be mindful to avoid malicious uses. When we release code and models, we would set a safeguard by requiring that users adhere to usage guidelines.

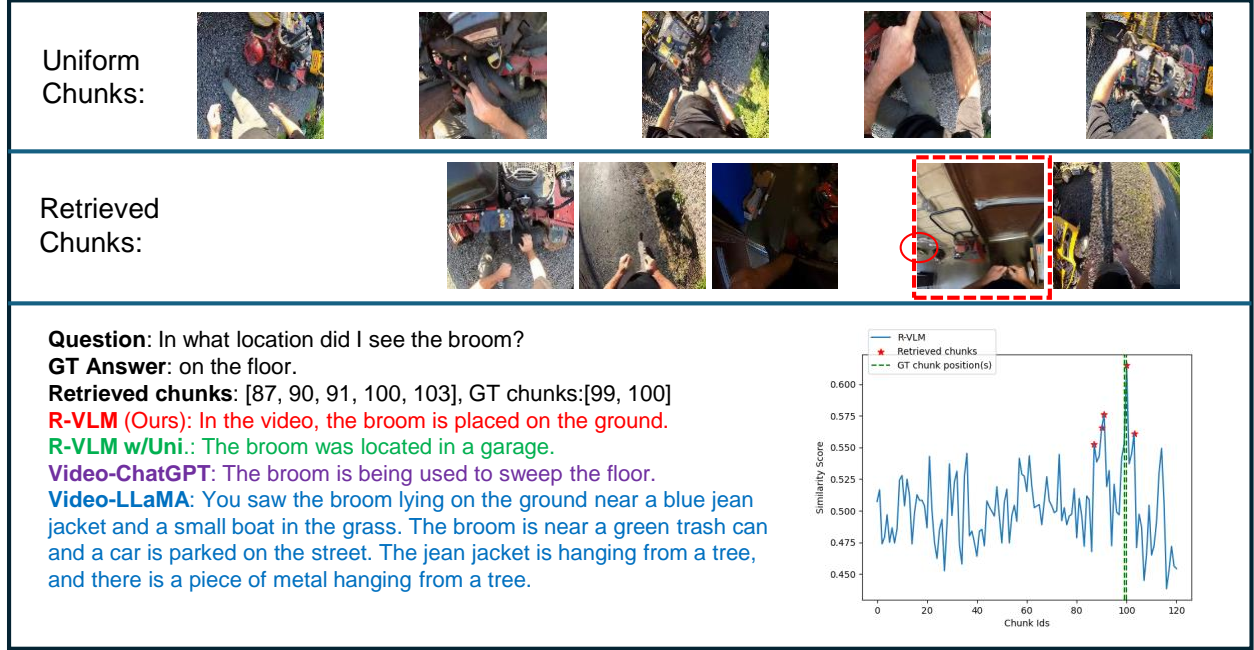


Fig. 4: Visualization of a video QA example from QAEgo4D. The broom is small and is on the left in the red boxed image. Our R-VLM captures exactly where the broom is, *i.e.*, on the ground. R-VLM w/Uni. does not capture the video chunks with broom and thus does not answer accurately. The answer of Video-ChatGPT is irrelevant to the question. The answer from Video-LLaMA is redundancy and tedious, where the mentioned blue jean jacket and boat actually do not appear in the video.

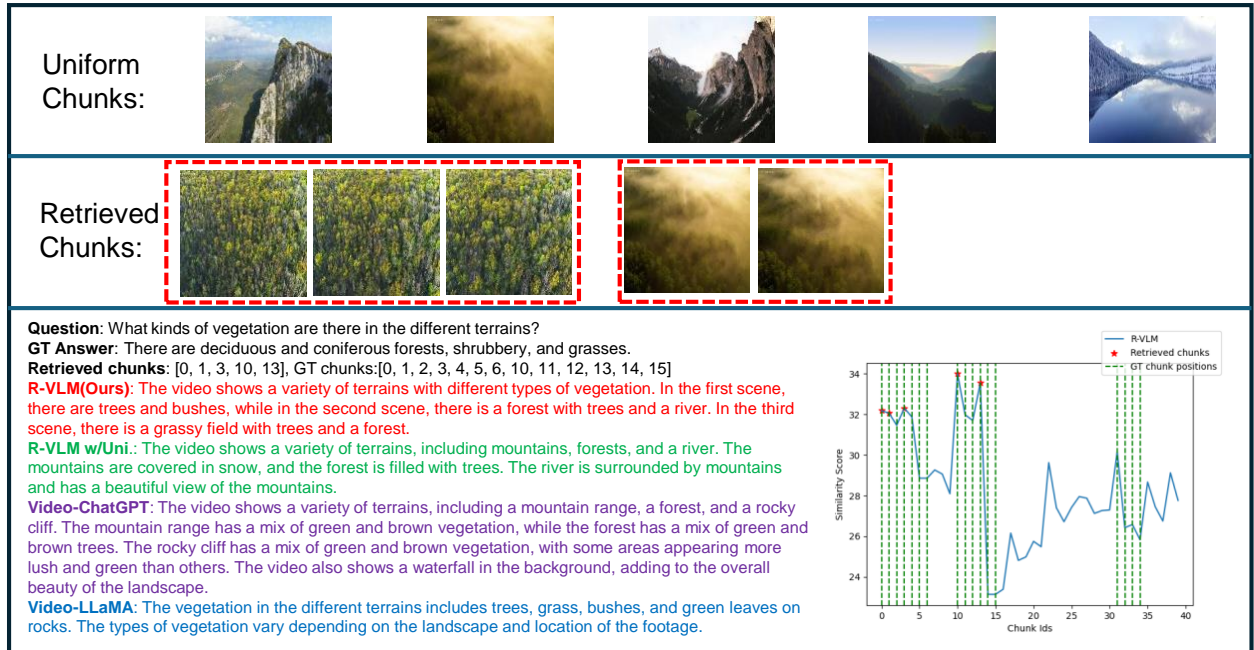


Fig. 5: Visualization of video QA examples from WildQA. In this video, two clips show vegetation and the remaining clips show mountains, rivers, *etc*. Uniform sampling mainly obtains segments such as mountains and rivers rather than segments with vegetation. Therefore, only the terrain was answered, without giving vegetation types. In contrast, our retrieved chunks contain video clips of vegetation. Thus the types of vegetation are predicted correctly: trees, bushes, forest. Video-ChatGPT gives a global description and does not answer specific vegetation types.

| | |
|---|--|
| Groundtruth Chunks: | |
| Retrieved Chunks: | |
| <p>Question: What is the man using the fire for? GT Answer: Based off the man using a stick to coax the pottery object out of the fire, I am assuming he used the fire to harden the object that was left in the fire for more than an hour. R-VLM (Ours): The man is using the fire to cook food.</p> | |

Fig. 6: A failure case from WildQA. This is a video of a person firing art. Although our R-VLM retrieved the correct chunks, it gave the wrong answer of “cook food”. This maybe caused by the visual ambiguity of the target object and the biases of the LLM.

| | |
|---|--|
| Groundtruth Chunks: | |
| Retrieved Chunks: | |
| <p>Question: What type of animals are there? GT Answer: dolphins, human, seagulls. R-VLM (Ours): There are two animals in the video.</p> | |

Fig. 7: A failure case from WildQA. Groundtruth chunks correspond to the chunks where three types of animals present, namely dolphins (the first chunk), seagulls, and human. Our method only retrieved the seagull and human chunks, but missed the dolphin chunk. R-VLM provided wrong answer due to the imperfect retrieval and the unsatisfactory reasoning capability of the used LLM.

| | |
|---|--|
| Groundtruth Chunks: | |
| Retrieved Chunks: | |
| <p>Question: Who did I talk to in the workshop? GT Answer: woman. R-VLM (Ours): In the workshop, you had a conversation with a man who was working on a project.</p> | |

Fig. 8: A failure case from QAEgo4D. Our method did not find the correct chunks. Therefore, large language model did not correctly answer the question and provided hallucinated answer.

Fig. 9: Visualization of failure cases from WildQA and QAEgo4D.